Effect of Cross-Links Which Occur during Continuous Chemical Stress-Relaxation†

Kenneth T. Gillen

Sandia National Laboratories, Albuquerque, New Mexico 87185. *Received June 15, 1987; Revised Manuscript Received August 31, 1987*

ABSTRACT: Large radiation-induced stress *increases* observed during the continuous stress-relaxation of a nitrile rubber aged in an inert, γ-radiation environment are analyzed using a simple (no adjustable parameters) shrinkage model derived from linear viscoelasticity. Stress-relaxation experiments based on the model in conjunction with determinations of the time-dependence of the material's modulus and linear shrinkage show that the observed increases in stress can be quantitatively accounted for by shrinkage effects caused by new cross-links. In contrast to typical assumptions, the results therefore show that new chemical cross-links formed during continuous stress-relaxation studies can have a large impact on the relaxation results. By using the model in conjunction with stress-relaxation experiments conducted as a function of initial sample strain, estimates can be made of the importance of shrinkage effects for any elastomer.

Introduction

In continuous chemical stress-relaxation experiments, it is important to understand whether the results are influenced by new chemical cross-links which form. Continuous stress-relaxation experiments are clearly sensitive to scission processes but are usually assumed to be insensitive to new cross-links, since such cross-links form at equilibrium in the stretched state and therefore do not contribute to the force being monitored.[1] Stress increases during continuous stress-relaxation experiments were observed in a number of studies and prompted an examination of this critical assumption. Tobolsky and coworkers[2,3] found increases in stress of *cis*-polybutadiene samples thermally aged under vacuum. Since they did not observe measurable sample shrinkage, they proposed that the stress was unaffected by cross-linking of free chains but increased due to the fraction of new cross-links occurring between stretched network chains. They claimed that the latter would bring network chains together without affecting the average extension ratio. Thus the stress was postulated to increase in the absence of sample shrinkage. Murakami and Ono[3] reported similar results for air-oven aging of a cross-linked polyester material in which continuous stress-relaxation experiments gave stress increases in the absence of measurable sample shrinkage. Yoshinari and Murakami[4] found a large stress increase for poly(isobutylene) UV aged in air but little increase for the same material UV aged in nitrogen. They attributed the increase to shrinkage resulting from oxidative degradation.

We have designed and built a new, unique stress-relaxometer, which allows us to separate irreversible chemical effects from reversible physical effects[5] during long-term combined thermal/high-energy radiation stress-relaxation experiments. While studying the chemical stress-relaxation in nitrogen of a nitrile rubber material exposed to a γ-radiation environment, we observed dramatic increases in stress. The dependence of this increase on time and initial strain was very similar to the results observed for the *cis*-polybutadiene[2,3] and the cross-linked polyester[3] materials. Through the use of a simple shrinkage model coupled with experimental determinations of (1) sample shrinkage from weight and density changes and (2) the dependence of modulus on the radiation dose, we are able to quantitatively show that the increase is due to sample shrinkage caused by γ-radiation induced cross-linking. Our results imply that when cross-linking dominates scission, very little shrinkage (a few tenths of 1%) is necessary to account for large relative stress increases at low values of initial strain. Such small values of shrinkage could easily have been missed in the earlier studies[2,3] which observed and modeled stress increases in the absence of measurable shrinkage. Since our model is general, it offers a universal method for estimating the importance of new cross-links on chemical stress-relaxation experiments, even for the vast majority of cases where increases in stress are not observed.

† This work performed at Sandia National Laboratories supported by the U.S. Department of Energy under Contract DE-AC04-76DP00789.

Experimental Section

Material. Nitrile rubber refers to formulations based on copolymers of acrylonitrile and butadiene. The material used in this study was a standard proprietary compound, designated N741-75, obtained from Parker Seal as 15 cm × 15 cm compression-molded sheets. Nominal sheet thickness was 0.95 mm. Rectangular samples approximately 13 cm long by 0.56 cm wide were cut and used for the stress-relaxation experiments. Very accurate estimates of the initial sample cross-sectional area (better than ±0.5%) were obtained by dividing the sample weight by the product of density (1.218 g/cm^3) and sample length.

Radiation-Aging Exposures. Radiation-aging exposures were carried out in a cobalt-60 facility which has been described in detail elsewhere.[6] The cobalt-60 is located in stationary racks at the bottom of a water-filled tank. Cylindrically shaped (~18-cm outside diameter) water-tight test cells, which are lowered into cylindrical holders at the bottom of the tank, allow for convenient, long-term aging exposures.

Stress-Relaxation Apparatus. The stress-relaxation experiments were conducted on a new, versatile and unique stress-relaxometer, which fits inside of a cylindrically-shaped (18-cm outside diameter, 65-cm length), double-walled (for thermal insulation), stainless-steel test cell. The stress-relaxometer, which is suspended from the lid of this water-tight test cell, is shown schematically in Figure 1. A Schaevitz Model FTA-G-1K (±1 kg) load cell is rigidly attached to a vertically movable holder. The holder is itself attached to the shaft of an Airpax L92411-P2 linear actuator (a stepper motor that has been modified by incorporating an internally threaded rotor fitted with a lead screw shaft). Two thredded rods are used to secure the actuator can to the test cell lid. The rigid frame, to which the bottom sample clamp is rigidly attached, is made up of two 1-cm-diameter thredded rods attached to the bottom of the actuator can and a base plate. The top sample clamp is rigidly attached to the load cell and therefore to the lead screw shaft of the linear actuator. Using this arrangement allows the use of the linear actuator to raise the upper clamp, thereby straining the sample.

A cylindrically shaped brass can (not shown) surrounds the sample region and is attached to the brass lid, shown in Figure 1. Heating of the sample region is achieved by using insulated nichrome wire wrapped around the sides of the brass can. Small holes in the brass lid allow access for temperature controlling and

0024-9297/88/2221-0442$01.50/0

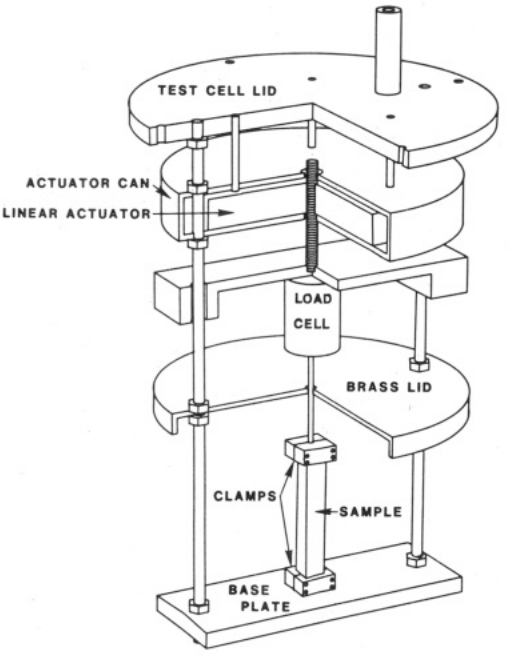

Figure 1. Schematic diagram of the stress–relaxometer.

monitoring thermocouples as well as clearance for the rod connecting the load cell to the top sample clamp. Between the brass lid and the load cell, the thredded rods support pancake reflectors and pieces of lead (neither shown), whose purpose is to lower the thermal and radiation stresses on the load cell and the linear actuator. At the moderate temperatures used so far (up to 50 °C), thermal stresses on the load cell and the linear actuator are minimal and have not caused problems. The reason for having these moderate temperature capabilities is the observation that ambient temperatures in the radiation source range from 22 °C (at the lowest dose rate of 0.02 kGy/h) to 48 °C (at the highest dose rate of ~7 kGy/h). Our temperature control capabilities therefore allow us to (1) isothermally assess the effects of radiation dose rate on stress relaxation and (2) isothermally turn on and off chemical relaxation effects by inserting the test cell into the radiation and removing it from the radiation, respectively.

A 2.9-cm outside diameter plastic tube is attached to the top of the test cell lid and runs up through the water tank to the surface electronics. Contained in this tube are control lines for the linear actuator, load cell, and heating tape, the monitoring and controlling thermocouple wires, and a gas flow tube which exits near the bottom of the sample. This latter feature allows us to conduct experiments under either air-flow or nitrogen-flow conditions.

At the start of an experiment, the sample is hung from the upper clamp and an accurate sighting device is used to measure the distance between two marks on the unstrained sample. After clamping, the brass heater can is attached, followed by the outer stainless-steel can. Gas flow is initiated and, if nitrogen is being used, allowed to flow through the system for a minimum of 1 day before the temperature is turned on. Once thermal equilibrium is reached (48 °C for the current experiments), the linear actuator is used to strain the sample in the absence of radiation, and the stress is monitored with a data logger. After the physical relaxation mechanism (reversible movement of strained chains toward equilibrium) has slowed down (approximately 1 day for the current experiments), the apparatus is lowered into the radiation source at the desired dose rate. This procedure minimizes complications caused by the physical mechanisms, since it involves isothermally turning on the irreversible chemical mechanisms only after the physical mechanisms have essentially died out.

Dividing $F(t)$, the time-dependent force from the LVDT, by the cross-sectional sample area, A (see Material), gives the time-dependent stress, $\sigma(t)$. The time-dependent modulus can then be obtained from

$$E(t) = \frac{3\sigma(t)}{\lambda - \lambda^{-2}} \quad (1)$$

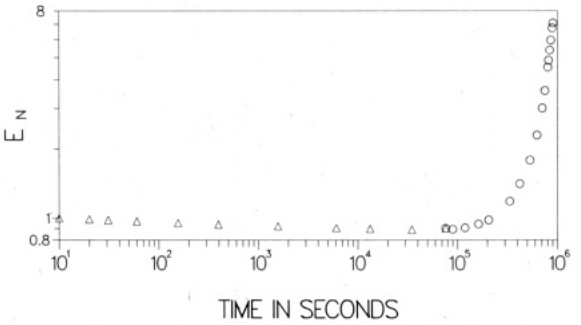

Figure 2. Stress–relaxation data normalized to the 10-s value for a nitrile rubber sample aged at 48 °C in nitrogen. The stretch ratio, $\lambda = 1.0193$ and the triangles show the results before the apparatus is transferred isothermally to the γ-radiation source at a dose rate of 7.35 kGy/h. The circles show the results after the transfer.

once the sample extension ratio, λ, is determined. At the end of the experiment, the temperature is turned off and the distance between marks on the strained sample, d_f, is measured at room temperature. To estimate the λ of interest (e.g., appropriate to the elevated-temperature experiment), we normally divide d_f by the room temperature unstrained distance between marks corrected for the thermal expansion which occurred when the sample temperature was raised prior to straining the sample. This procedure was used for the high-strain experiment ($\lambda = 1.114$), but its reliability becomes questionable as the strain is reduced to a few percent. For the lower strain experiments we therefore used another indirect method of estimating λ. It is based on the observation[7] that the modulus of this material is independent of the imposed strain, as expected for linear, viscoelastic materials. We therefore assumed that all samples have identical values of the modulus just prior to introducing them into the radiation environment (~1 day after straining). The value used was $E(1\ \text{day}) = 7.1$ MPa, obtained from the $\lambda = 1.114$ experiment. This value of $E(t)$ together with the accurately known values of $\sigma(t)$ allowed us to use eq 1 to estimate λ values for the low-strain experiments.

Modulus Measurements. Modulus measurements were made on samples after completion of the stress–relaxation experiments and, for comparison, on unstressed samples radiation aged at 48 °C in nitrogen at various doses. The technique used involved an updated version[7] of a quantitative penetration approach.[8] This method, which yields the inverse of the tensile compliance (closely related to the modulus) from the measured penetration of a weighted paraboloid of revolution, was chosen for a number of reasons. First, having only one stressed sample per radiation aging condition meant that using a technique capable of repeated measurements on one sample was advantageous. An additional advantage of the technique is its ability to estimate modulus values at low frequencies (longer times), i.e., after the initial rapid decay of the modulus in the first few seconds. In this paper, we used the penetration technique to measure the modulus after 2 min.

Shrinkage Measurements. Very accurate estimates of volume shrinkage for mechanically stressed and unstressed samples exposed to radiation were obtained from measurements of the weight and density changes of the samples. Density measurements were made by using a $CaNO_3$–H_2O density gradient column, with estimated uncertainty less than ± 0.001 g/cm^3. Weight changes, monitored with a precision balance, were insignificant; thus the volume changes were inversely related to the density changes.

Results and Discussion

Figure 2 shows typical stress–relaxation data for the nitrile rubber material aged at 48 °C in nitrogen. The time dependence of the normalized tensile modulus, $E_N(t)$, which is defined as $E(t)/E(10\ \text{s})$, is plotted versus the time in seconds. For the first time 7.6×10^4 s (~21 h) after straining (stretch ratio $\lambda = 1.0193$), the material physically relaxed in the absence of radiation (data shown with triangles). After 7.6×10^4 s, when the physical relaxation

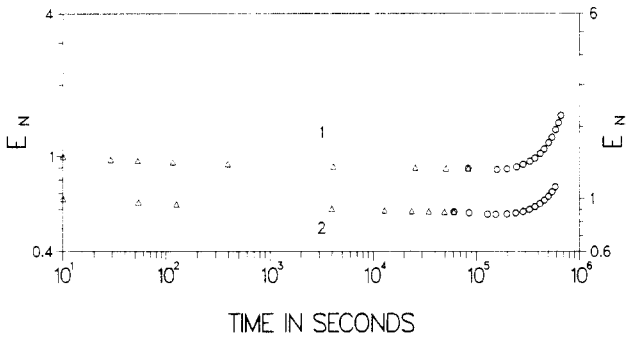

Figure 3. Normalized stress–relaxation data for samples with higher initial stretch ratios than the sample in Figure 1. The curve labeled 1 has $\lambda = 1.0538$; the curve labeled 2 has $\lambda = 1.114$ and is displaced downward (vertical axis on right side of figure) for ease of viewing.

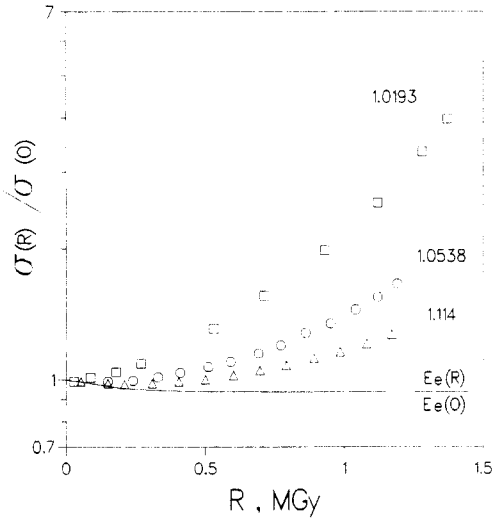

Figure 4. Normalized stress results (relative to value when first placed in radiation) versus radiation dose, R, for the data shown in Figures 2 and 3. Squares, circles, and triangles denote the data appropriate to the indicated sample extension ratios. The solid curve gives the normalized results derived from eq 7.

had significantly slowed down, the apparatus was transferred isothermally into the γ-radiation source at a dose rate of 7.35 kGy/h (1 Gy = 100 rad). Once the chemical effects were turned on by the radiation, the modulus (stress) increased dramatically, eventually reaching 7 times the initial value when the experiment was terminated after 9.5 days of radiation. The data shown by circles cover the time span when the apparatus was in the radiation environment. Figure 3 shows results for similar experiments, but with larger stretch ratios. Increases in stress are also observed for these experiments once the radiation is turned on, but the amount of increase is lowered as the stretch ratio is increased. The data plotted as squares, circles, and triangles in Figure 4 represent the radiation portion of the data from Figures 2 and 3, where the normalized stress (normalized to the value when the sample is first introduced into the radiation) is plotted versus the radiation dose. The qualitative behavior of this data is very similar to Tobolsky's[2,3] stress–relaxation results for *cis*-polybutadiene in vacuum ovens and Murakami's[3] stress–relaxation results for cross-linked polyester in air ovens.

Measurements of density and weight changes caused by the radiation showed that the radiation caused substantial sample shrinkage. For example, after 1.68 MGy, the density increased by ~4% while the weight remained constant, implying a volume shrinkage of 4%. We will show below that the dramatic stress increases observed for the nitrile material can be quantitatively accounted for by the observed shrinkage. We begin by defining the strain in the sample, S, as

$$S = \frac{\lambda - \lambda^{-2}}{3} \tag{2}$$

The relationship between the stress, σ, and the strain comes from linear viscoelasticity in which the appropriate constitutive equation[9] is based on the principle that the effects of sequential changes in strain are additive,

$$\sigma(t) = \int_{-\infty}^{t} E(t - t') \frac{dS(t')}{dt'} dt' \tag{3}$$

where $E(t - t')$ is the relaxation modulus and the integration is carried out over all past times t' up to the current time t. For our experiments, we put an initial strain S_0 on the sample at time zero and then allow it to physically relax for approximately 1 day before transferring the sample into radiation at time t_γ. Assuming the initial sample modulus is close to its equilibrium value, E_e, at the moment of transfer into radiation, eq 3 gives[9]

$$\sigma(t_\gamma) = E_e S_0 \tag{4}$$

If shrinkage does not occur (the normal assumption) after the sample is placed in the radiation, $\sigma(t)$ will decrease due to scission effects occurring with time or equivalently with radiation dose, R. This gives

$$\sigma(t - t_\gamma) = \sigma(R) = E_e(R) S_0 \tag{5}$$

where $E_e(R)$ is the equilibrium modulus for the initial material reduced by the radiation-induced scission processes.

When shrinkage effects are important, we assume that they are equivalent to sequential changes in strain acting on the modulus value appropriate to the time at which the incremental change in strain occurs. This leads to

$$\sigma(R) = E_e(R) S_0 + \int_0^R E[\nu(R'),R-R'] \frac{dS(R')}{dR'} dR' \tag{6}$$

where $E[\nu(R'),R-R']$ is defined as the modulus existing after a dose R' (different from initial modulus due to cross-linking and scission caused by the radiation dose), reduced by scission effects occurring from R' to R. When the shrinkage effects become larger than the drop in the first term on the right-hand side of eq 6, the stress will begin to increase with dose, as found for the present material.

With the assumption that $E[\nu(R'),R-R']$ and $dS(R')/dR'$ are independent of the initial strain, S_0, a reasonable first approximation for small initial strains, the integral on the right-hand side of eq 6, will depend only on the dose R. This gives

$$\sigma(R) = E_e(R) S_0 + I(R) \tag{7}$$

By following the stress versus dose at a minimum of two different initial strains, eq 7 can be used to obtain $E_e(R)$ and $I(R)$. If, as is true in the present case, data from experiments at three or more strains are available, the predicted linearity of the data according to eq 7 can be checked. Smooth curves thru the unnormalized data used to obtain the Figure 4 points were analyzed in this fashion. Representative plots of $\sigma(R)$ versus S_0 at doses R of 0.1, 0.4, 0.8, and 1.15 MGy are shown in Figure 5. The apparent linearity of the plots offers good evidence for the assumptions used to derive eq 7. From eq 7, the slopes and intercepts from such plots yield $E_e(R)$ and $I(R)$. The solid curve of Figure 6 plots the dependence of $I(R)$ on the dose R, and the normalized results for $E_e(R)$ are plotted in Figure 4 (solid curve). The dependence of E_e on R

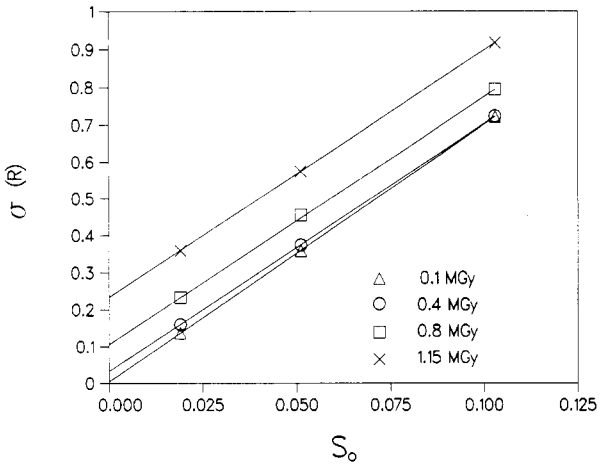

Figure 5. Stress–relaxation data at three different initial strains, S_0, analyzed according to eq 7. Stress data after 0.1, 0.4, 0.8, and 1.15 MGy radiation dose is plotted versus S_0.

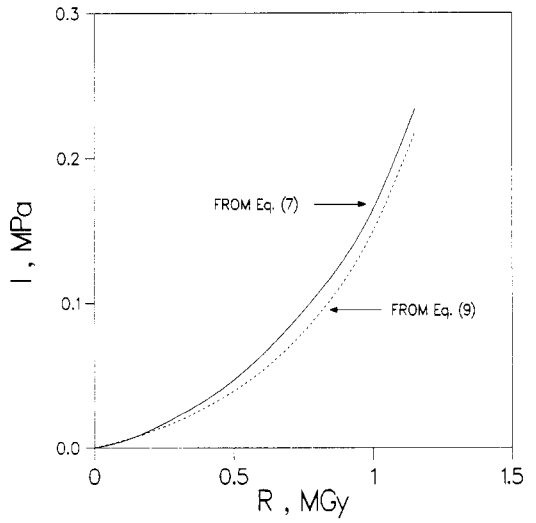

Figure 6. Derived values of I plotted versus the radiation dose, R. The solid curve comes from eq 7, the dashed curve from eq 9.

predicts the stress–relaxation which would have occurred in the absence of cross-linking-induced shrinkage. It therefore represents the effects of scission and any remaining physical relaxation on the initial modulus. Since E_e only drops a few percent, it is clear that scission effects are insignificant for this nitrile rubber aged in an inert γ-radiation environment. Cross-linking, on the other hand, is extensive, as evidenced by the large increases in modulus measured on the materials after completion of aging (Figure 7). Since crosslinking so dominates the degradation, it is not surprising that important shrinkage effects occur. The data in Figure 7 also show that the modulus does not appear to depend on the strain present during radiation, offering further evidence for one of the assumptions used to arrive at eq 7.

The above analysis is predicated on the use of an equation which was derived by assuming shrinkage effects are responsible for the observed anomalous stress–relaxation results. To confirm this we will now compare the values of I resulting from the above analysis (solid curve in Figure 4) with estimates of the integral derived directly from its definition in eq 6, e.g., from

$$I(R) = \int_0^R E[\nu(R'),R-R'] \frac{dS(R')}{dR'} dR' \qquad (8)$$

$E[\nu(R'),R-R']$ represents the equilibrium modulus after a

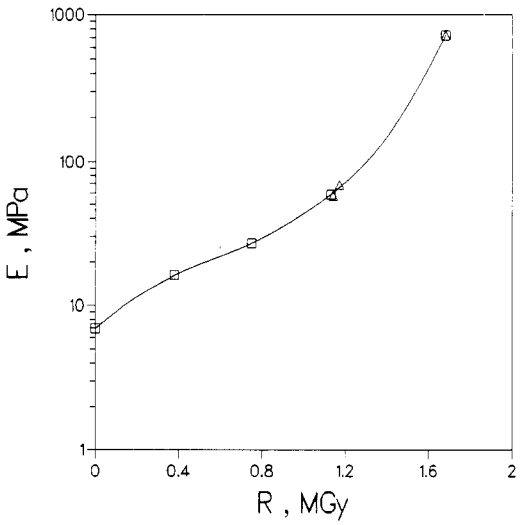

Figure 7. Modulus values plotted versus the radiation dose. Squares denote data taken on samples which were radiation aged at 48 °C in nitrogen in the absence of mechanical stress; triangles denote data taken on samples after completion of aging under mechanically stressed conditions.

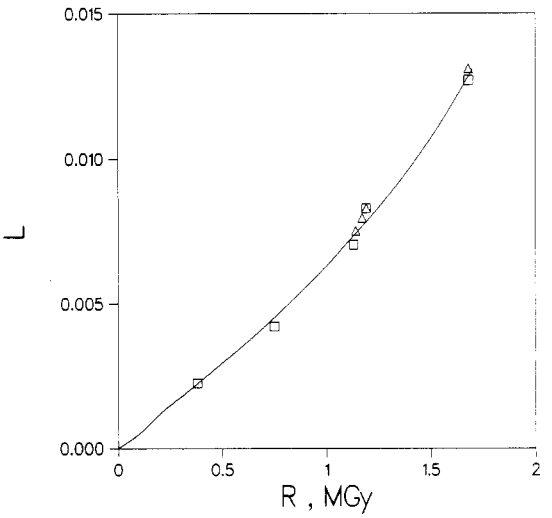

Figure 8. Fractional linear shrinkage, obtained from weight and density changes, plotted versus the radiation dose. Squares denote data for samples which were radiation-aged in the absence of mechanical stress; triangles are for samples which were mechanically-stressed during aging.

dose R' reduced by scission and physical relaxation processes occurring during the time interval required for the dose to increase from R' to R. Since the Figure 4 results imply that these processes reduce E_e by a negligible amount (when E is small), it is reasonable to assume that they remain negligible as the cross-link density increases, i.e., as E increases with dose. This implies that $E[\nu(R'),R-R'] \sim E[\nu(R')]$ which gives

$$I(R) \sim \int_0^R E[\nu(R')] \frac{dS(R')}{dR'} dR' \qquad (9)$$

To estimate $E[\nu(R')]$, we use the modulus results shown in Figure 7. For values of $dS(R')/dR'$, we first need to estimate the dependence of linear shrinkage on the radiation dose. Assuming that the volume shrinkage obtained from the density changes (weight changes were negligible) is isotropic, the density measurements lead to the linear shrinkage results shown in Figure 8. These data immediately allow the shrinkage strain to be calculated versus R and therefore $dS(R')/dR'$ versus R. Combining the latter results with the estimates of $E[\nu(R')]$ and integrating the

product according to eq 9 give $I(R)$ versus R. These predictions are indicated by the dashed curve in Figure 6. The agreement with the values of I derived earlier from eq 7 is excellent, offering confirmatory evidence for the suggested model. Thus the rather striking stress increases observed in Figures 2 and 3 can be almost totally and quantitatively accounted for by shrinkage effects. By comparing Figures 4 and 7, it can be seen that relatively small amounts of shrinkage can result in very large anomalous behavior, especially for small initial sample extension ratios.

Although this paper analyzes a case where cross-linking so dominates scission that large stress increases occur, the methods described can be used to eliminate shrinkage effects for more typical situations where the amount of cross-linking may not be sufficient to cause the stress to increase. Whenever the normalized stress-relaxation of an elastomeric system is found to depend on the initial strain S_0, eq 7 can be used to estimate $E_e(R)$ and $I(R)$ or equivalently $E_e(t)$ and $I(t)$. The resulting values of $E_e(t)$ will then give the predicted stress-relaxation results in the absence of cross-linking-induced shrinkage. In the current paper, the physical relaxation was allowed to approach equilibrium before radiation-induced shrinkage was initiated, a procedure which permits one to more directly ascertain scission-induced effects. For stress-relaxation studies in high-temperature environments, such an approach is not possible. However, as long as thermally aged samples are strained rapidly compared to the rate of shrinkage-induced strain, eq 6 and 7 can still be applied. The derived values of $E_e(t)$ will then give the stress-relaxation caused by a combination of physical relaxation and scission. The values of $I(t)$ obtained in the analysis can then be independently verified by using eq 8 if appropriate modulus and shrinkage values are available. Shrinkage estimates can usually be made from density and weight changes. When scission and physical effects are minor, such as for the current material, estimates of the appropriate modulus values are also possible. On the other hand, for materials with significant scission effects, the assumption that $E(t - t') \sim E(t')$ cannot be made, making it more difficult to use eq 8 to verify the values of I obtained from eq 7. We are currently working on material which fits into this category with the intent of determining the effects that significant scission has on the use of eq 8.

Acknowledgment. I gratefully acknowledge J. G. Curro for helpful discussions on viscoelasticity, L. H. Jones for help in designing and constructing the apparatus, and N. J. Dhooge for assistance in apparatus construction and data generation.

References and Notes

(1) Andrews, R. D.; Tobolsky, A. V.; Hanson, E. E. *J. Appl. Phys.* **1946**, *17*, 352.
(2) Tobolsky, A. V.; Takahashi, Y.; Naganuma, S. *Polym. J.* **1972**, *3*, 60.
(3) Murakami, K.; Ono, K. *Chemorheology of Polymers*; Elsevier Scientific: Amsterdam, 1979.
(4) Yoshinari, M.; Murakami, K. *J. Polym. Sci., Polym. Chem. Ed.* **1979**, *17*, 3307.
(5) Curro, J. G.; Salazar, E. A. *J. Appl. Polym. Sci.* **1975**, *19*, 2571.
(6) Gillen, K. T.; Clough, R. L.; Jones, L. H. *Sandia National Laboratories Report, SAND 81-2613*, August, 1982.
(7) Gillen, K. T.; Clough, R. L.; Quintana, C. A. *Polym. Degrad. Stabil.* **1987**, *17*, 31.
(8) Gillen, K. T. *J. Appl. Poly. Sci.* **1978**, *22*, 1291.
(9) Ferry, J. D. *Viscoelastic Properties of Polymers*, 2nd ed.; Wiley: New York, 1970.

Distribution of Interactions in Binary Polymer Mixtures: A Monte Carlo Simulation Study

Peter Cifra,† Frank E. Karasz,* and William J. MacKnight

Department of Polymer Science and Engineering, University of Massachusetts, Amherst, Massachusetts 01003. *Received June 23, 1987*

ABSTRACT: Phase transitions from miscibility to immiscibility were observed in simulations of binary polymer mixtures on a planar square lattice using reptation sampling techniques. The relationship between the phenomenological interaction parameter, χ, and the true molecular interaction energy was followed, and the dependence of the number and distribution of heterocontacts in the mixture on the applied heterosegment interaction energy was determined. Deviations from the results of mean-field treatments, which overestimate the number of heterocontacts, were observed even for athermal mixtures. Kinetically driven hysteresis governed by a temperature equilibration time scale was examined for the phase transitions. An important prediction of expansion of the polymer chains in the miscibility region can be made on the basis of the results of chain end-to-end distance calculations.

Introduction

The subject of polymer blends has been studied extensively[1] mainly as a result of the potential applications of polymer blends as new materials. For each particular blend the question of miscibility and immiscibility arises. In general, miscibility is unusual for blends of high molecular weight polymers. The Gibbs free energy of mixing, which governs phase behavior, consists of three contributions: an exchange interaction term, the combinatorial entropy of mixing, and a free volume term. The basic term is considered to be the exchange interaction term. A prerequisite for miscibility is that the energy of mixing be endothermic. The combinatorial entropy of mixing is very small due to the large size of polymeric molecules. The free volume term, which is unfavorable to mixing, also has a relatively small effect at low or moderate temperatures in polymer-polymer systems since differences in the sizes of the molecules, and hence differences in the free volumes are small, unlike polymer-solvent systems. It is highly desirable to follow in detail the number of favorable/unfavorable heterocontacts in the mixture and also to determine the distribution of unlike contacts. It should be

† Permanent address: Polymer Institute, Slovak Academy of Sciences, 842 36 Bratislava, Czeckoslovakia.

0024-9297/88/2221-0446$01.50/0